REPORT PR11455

LEVEL II

12

DESIGN AND PERFORMANCE EVALUATION OF SUPERCRITICAL AIRFOILS FOR AXIAL FLOW COMPRESSORS

UNITED TECHNOLOGIES CORPORATION
Pratt & Whitney Aircraft Group
Government Products Division
P. O. Box 2691
West Palm Beach, Florida 33402

JUNE 1979

FINAL REPORT

PREPARED FOR

DEPARTMENT OF THE NAVY
NAVAL AIR SYSTEMS COMMAND
WASHINGTON, DC 20361

UNCLASSIFIED

SECURITY CLASSIFICATION OF THIS PAGE (When Data Entered)

REPORT DOCUMENTATION PAGE

READ INSTRUCTIONS BEFORE COMPLETING FORM

1. REPORT NUMBER: FR 11455
2. GOVT ACCESSION NO.:
3. RECIPIENT'S CATALOG NUMBER:

4. TITLE (and Subtitle): (6) DESIGN AND PERFORMANCE EVALUATION OF SUPERCRITICAL AIRFOILS FOR AXIAL FLOW COMPRESSORS.

5. TYPE OF REPORT & PERIOD COVERED: (9) Final rept.

6. PERFORMING ORG. REPORT NUMBER:

7. AUTHOR(s): (10) Stephens, H.E./Stephens; Hobbs, D.E./Hobbs

8. CONTRACT OR GRANT NUMBER(s): (15) N00019-77-C-0546

9. PERFORMING ORGANIZATION NAME AND ADDRESS:
Pratt & Whitney Aircraft Group
Government Products Division P.O. Box 2691
West Palm Beach, Florida 33402

10. PROGRAM ELEMENT, PROJECT, TASK AREA & WORK UNIT NUMBERS: (11) Jan. '79

11. CONTROLLING OFFICE NAME AND ADDRESS:
Naval Air Systems Command
Washington, D.C. 20361

12. REPORT DATE: February 1979

13. NUMBER OF PAGES: 42

14. MONITORING AGENCY NAME & ADDRESS (if different from Controlling Office): (12) 46p.

15. SECURITY CLASS. (of this report): Unclassified

15a. DECLASSIFICATION/DOWNGRADING SCHEDULE:

16. DISTRIBUTION STATEMENT (of this Report)

Approved for public release; distribution unlimited.

(14) PWA-FR-11455

17. DISTRIBUTION STATEMENT (of the abstract entered in Block 20, if different from Report)

18. SUPPLEMENTARY NOTES

19. KEY WORDS (Continue on reverse side if necessary and identify by block number)

Supercritical Airfoil
Transonic Cascade Tunnel
Fan Exit Stator
Computer Design
Turbulent Boundary Layer
Laminar Boundary Layer
Light Pen Scope
Compressor
Shockless Airfoils

20. ABSTRACT (Continue on reverse side if necessary and identify by block number)

Pratt & Whitney Aircraft has developed an analytical design procedure for producing supercritical cascade airfoils satisfying practical aerodynamic and structural requirements. The purpose of this research is to demonstrate the potential for substantial efficiency improvements in compressor stages incorporating these airfoil designs.

DD FORM 1 JAN 73 1473 EDITION OF 1 NOV 65 IS OBSOLETE

DW

UNCLASSIFIED

SECURITY CLASSIFICATION OF THIS PAGE (When Data Entered)

392 887

20

The midspan section of a fan exit stator was selected for the design application. An airfoil was designed, fabricated, and tested in a transonic cascade tunnel. Test conditions were varied over a wide range of inlet flow angles and inlet Mach numbers to determine design and off-design performance. Test point information included inlet and exit conditions and airfoil surface pressure distribution.

Analysis of test data taken at the design point conditions substantiates a good match between measured and design shockless surface Mach number distribution, a low loss resulting from an attached suction side boundary layer, and an exit flow angle within one degree of design specifications. Thus design goals were successfully met. Analysis of test results for off-design conditions confirmed that the cascade also operates efficiently over a wide range of inlet angles and Mach number. The validity of the Pratt & Whitney Aircraft supercritical design procedure has been demonstrated.

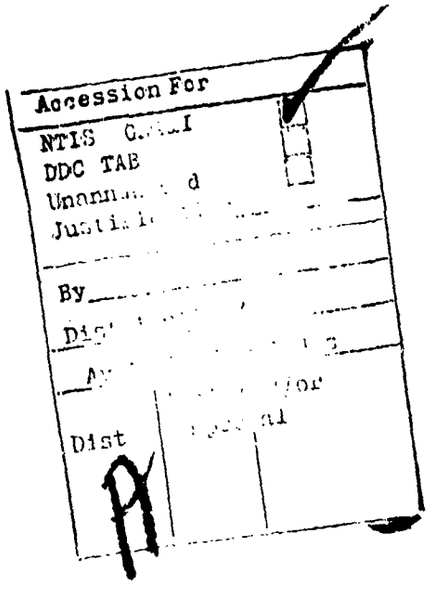

TABLE OF CONTENTS

LIST OF ILLUSTRATIONS

LIST OF ILLUSTRATIONS (Cont.'d)

1.0 INTRODUCTION

This report discusses the details of the design and the performance evaluation of a practical supercritical cascade. The purpose of this work is to demonstrate that potentially substantial improvements in compressor efficiency can result from employment of analytically designed, shockless supercritical airfoils. Conventional compressor airfoils operating in the transonic regime typically exhibit high losses, which are principally combinations of shock losses and shock-induced boundary layer separation losses. Recent Pratt & Whitney Aircraft experience in the development and test of supercritical airfoils in cascades has demonstrated the superiority of these airfoil designs over conventional compressor airfoil designs in terms of both reduced losses and increased incidence range. This contract provides for the design, test, and data analysis of a supercritical cascade for application in high technology, future generation compressors of gas turbine engines.

2.0 BACKGROUND

2.1 Development of Supercritical Airfoil Design Methods

Supercritical airfoils are a class of transonic airfoils which operate with subsonic inlet and exit flow velocities and with embedded regions of supersonic flow adjacent to the airfoil surface. The term "supercritical" refers to the presence of velocities in the flow field which are above the "critical" or sonic speed. Historically, progress in the design methods for transonic airfoils has severely lagged methods used to design fully subsonic or supersonic airfoils. This lag is primarily due to the mathematical difficulties in solving the equations which model the transonic flow field. Without the fundamental ability to compute the velocities on the airfoil surface, the well-developed low speed design techniques employing boundary layer theory have been of no value.

The early knowledge of airfoils in the transonic regime was derived from wind tunnel experiments on subsonic or supersonic designs. This type of experimentation provided an understanding that aerodynamic deficiencies of these designs were caused by the strong normal shocks which terminated the embedded supersonic region. For isolated airfoils, this shock caused a rapid increase in drag and a reduction of lift as the approach Mach number increased through the high subsonic range. In cascades, this shock produced the analogous effects of increased total pressure loss and reduced flow turning. These features of the flow field for a NACA 65 series cascade are shown in the schlieren photographs in Figure 1 from the work of Dunavant et.al. (1).

In 1965, a resurgence of interest in developing improved supercritical design methods resulted from Whitcomb's now-famous supercritical isolated airfoil experiment in the NASA Langley eight-foot transonic tunnel. Whitcomb's experimentally developed airfoil demonstrated the existence of shockless supercritical flow fields (2). The shockless feature made the flow entirely irrotational and thus amenable to modelling with the potential equation.

---

1. Dunavant, J. C. et. al. "High Speed Cascade Tests of the NACA 65-($12A_{10}$)10 and NACA 65-(12 A_2I_8b)10 Compressor Blade Sections," NACA RML55, 108.

2. Whitcomb, Richard T., and Clark, Larry R., "An Airfoil Shape for Efficient Flight at Supercritical Mach Numbers," NASA TMX-1109, May 1965.

Subsequently, Garabedian, Korn and Bauer (3, 4, and 5) of New York University developed a complex hodograph solution satisfying the two-dimensional potential equation for supercritical flows over isolated airfoils. By using this hodograph technique, an isolated airfoil shape could be determined from a specified shockless surface velocity distribution. The final design program, including viscous boundary layer considerations, was delivered to NASA in 1974, and has been used to design airfoils for a variety of applications. In the same year, Korn (6) developed a shockless supercritical cascade design system. In a cooperative program with Pratt & Whitney Aircraft, a supercritical cascade was designed in 1974 by Korn, and tested in 1976 in the transonic cascade facility of the DFVLR (Deutsche Forschung and Versuchsanstalt fur Luft und Raumfahrt). The airfoil is shown in Figure 2. The analysis of the results of this test (7) validated the new design methods, including the shockless feature of the flow field, the near match of the design surface velocity distribution, and the attached viscous boundary layer. The Korn design also showed good performance at both off-design and design conditions, indicating that the shocks, if present in the flow field at off-design conditions, were not a serious problem.

Although these test results demonstrated the feasibility of supercritical airfoil design, they did not demonstrate a practical compressor airfoil design capability because the existing hodograph design procedure provided structurally undesirable airfoil shapes and did not produce designs at arbitrary low cascade gap-to-chord ratios (non-dimensional airfoil spacing).

---

3. Bauer, Francis, Garabedian, Paul, and Korn, David, "Supercritical Wing Sections," Lecture Notes in Economics and Mathematical Systems, Vol. 66, Springer - Verlag, New York, 1972.

4. Bauer, Francis, Garabedian, Paul, Korn, David, and Jameson, Antony, "Supercritical Wing Sections II" Lecture Notes in Economics and Mathematical Systems, Vol. 108, Springer - Verlag, 1975.

5. Bauer, Francis, Garabedian, Paul, and Korn, David, "Supercritical Wing Sections III," Lecture Notes in Economics and Mathematical Systems, Vol. 150, Springer - Verlag, New York, 1977.

6. Korn, David, "Numerical Design of Transonic Cascades," ERDA Research and Development Report COO-3077-72, Courant Inst. Math. Sci., New York Univ., January 1975.

7. Stephens, Harry E., "Application of Supercritical Airfoil Technology to Compressor Cascades: Comparison of Theoretical and Experimental Results," AIAA Paper 78-1138, AIAA Fluid and Plasma Dynamics Conference, Seattle, Wash., July 1978.

These test results provided the motivation for the development of a practical transonic cascade design procedure by Pratt & Whitney Aircraft during 1976 and 1977. The current work was undertaken in November 1977 to demonstrate this new design system for practical applications to the compressor.

3.0 DESIGN

3.1 Design Procedure

The objective of the design process is to find an airfoil shape that satisfies a related set of aerodynamic and structural requirements. For supercritical cascade airfoils, these requirements can be briefly stated as follows.

1. The cascade must produce a specified exit velocity and flow angle for a specified inlet velocity and flow angle. The flow turning implied by these conditions should be accomplished with a minimum of total pressure loss through the cascade.

2. The cascade gap-to-chord ratio should be maximized (consistent with aerodynamic requirements on peak suction side Mach number) to reduce engine weight and cost.

3. The cascade airfoil must have a thickness and camber distribution capable of sustaining the aerodynamic pressure forces. Leading and trailing edges must be capable of sustaining erosion and foreign object damage.

To achieve these aerodynamic requirements, it is currently believed that the surface velocity distribution should have certain characteristics. These characteristics are listed below and summarized in Figure 3.

Supercritical cascade airfoil characteristics

1. A continuous acceleration to the peak Mach number on the airfoil suction surface, to avoid premature laminar boundary layer separation, or transition before the peak.

2. A peak Mach number less than 1.3 to avoid boundary layer separation induced by a severe shock wave-boundary layer interaction, should a shock develop at off-design conditions.

3. A continuous deceleration from the peak suction surface Mach number to the trailing edge, maintaining a

turbulent boundary layer with a low level of skin friction and avoiding separation ahead of the trailing edge.

4. A nearly constant subsonic Mach number distribution on the pressure surface.

The procedure developed at Pratt & Whitney Aircraft for designing a supercritical cascade that meets the preceding objectives requires an iteration among an inviscid transonic cascade flow calculation, a compressible integral boundary layer calculation, and a numerical smoothing calculation for the airfoil surface contour. This iteration is performed using an IBM 370-3033 computer system linked to an IBM 2250 light pen scope terminal, permitting designer interaction when necessary.

The designer starts the iteration with a transonic analysis of a preliminary airfoil. To achieve the desired surface velocity distribution, the designer then modifies the airfoil shape or gap-to-chord ratio. Airfoil contour changes are made by using the light pen scope. Complete flexibility is achieved by changing individual coordinates defining the airfoil surface. A smoothed alteration of the coordinates then produces a new airfoil, which is subsequently reanalyzed. When the resulting airfoil appears nearly correct, the computed boundary layer displacement thickness is superimposed on the airfoil surface during the transonic flow analysis iteration. The final design gas turning angle and total pressure loss is verified by a control volume wake mixing analysis.

The major computations used in this design system have been described in detail in the open literature. The transonic cascade analysis solutions are provided by Ives and Luitermoza (8, 9) and the boundary layer analysis solutions by McNally (10). The wake mixing calculation

---

8. Ives, David C., and Liutermoza, John F., "Analysis of Transonic Cascade Flow Using Conformal Mapping and Relaxation Techniques," AIAA Journal, Vol. 15, No. 5, May 1977, pp. 647-652.

9. Ives, David C., and Liutermoza, John F., "Second Order Accurate Calculation of Transonic Flow Over Turbomachinery Cascades," AIAA Paper 78-1149, AIAA 11th Fluid and Plasma Dynamics Conference, Seattle, Wash., July 1978.

10. McNally, W. D., "Fortran Program for Calculating Compressible Laminar and Turbulent Boundary Layers in Arbitrary Pressure Gradients," NASA TN D-5681, May 1970.

is of the type described by Lieblein (11) or Stewart (12). The transonic flow solution uses a second order accurate, finite difference scheme to solve the two-dimensional, fully non-linear, potential flow equation. The analysis also includes a quasi three-dimensional capability to account for the stream tube height variations through the cascade. This feature is essential for accurate modelling of realistic flow fields. With this analysis, supercritical flow fields can be computed for nearly all cascades of practical interest. The accuracy of this solution has been shown (9) to be equivalent to the Garabedian, Korn and Bauer cascade solution. The boundary layer analyses program of McNally includes the compressible, integral method of Cohen and Reshotko for laminar layers and the compressible, integral method of Sasman and Cresci for turbulent layers. Transition between the initially laminar layer and the turbulent layer is assumed to occur at the location of a computed laminar boundary layer separation. Smoothing of the boundary layer characteristics through transition is used to avoid discontinuities in the displacement thickness.

3.2 Design Description

The particular design application selected for this contract work is the midspan section of a fan exit stator. The Mach numbers, flow turning, and static pressure rise requirements are representative of advanced gas turbine engine configurations and reflect a design goal typical of current compressor airfoil technology. The selected design is also consistent with the requirements of the mean section of the exit stator of the 1600 ft/sec tip speed fan, previously designed and tested under NASA contract. The existence of this fan rig and its previously measured performance base line using a conventional stator provides future opportunity for an economical demonstration of a supercritical stator in a real turbomachinery environment. The stator design point aerodynamic requirements for inlet flow angle, inlet Mach number, and flow turning are taken from Table 10.10 of the NAS3-10482 contract report (13).

---

11. Lieblien, S., and Rouderbush, W. H., "Theoretical Loss Relations for Low Speed Two-Dimensional Cascade Flow," NACA TN 3662, March 1956.

12. Stewart, W. L., "Analysis of Two-Dimensional Compressible Flow Loss Characteristics Downstream of Turbomachine Blade Rows in Terms of Basic Boundary Layer Characteristics," NACA TN 3515, July 1955.

13. Sulam, D.H., M.S. Keenan, and J.T. Flynn, "Single-Stage Evaluation of Highly-Loaded Multiple-Circular-Arc Rotor High-Mach-Number Compressor Stages," NASA CR-7264, PWA-3772.

The performance requirements of the stator design include an inlet Mach number of 0.76, inlet flow angle of 46.8 degrees, and a flow turning of 43.2 degrees to an axial discharge angle. The design has an exit Mach number of 0.529, and a spanwise stream tube area contraction of 1.124.

The design parameter selection phase of the design iteration was performed using simple modifications of the Korn supercritical cascade airfoil and resulted in a choice of gap-to-chord ratio of 0.7. The computed peak suction surface Mach number was 1.27 and the diffusion factor was 0.54. This initial design was used to start the final design iteration resulting in the final cascade design (see Figure 4). A plot of an individual blade contour and the corresponding design surface Mach number distribution is presented in Figure 5. Smoothness quality of the computed Mach number distribution is dependent on the computational grid size employed in the transonic analysis and on airfoil contour variations with smaller than reasonable manufacturing tolerances. The large Mach number variations at the trailing edge are due to the computation of an inviscid stagnation point at the trailing edge. This stagnation point will not appear in the real flow because of strong viscous effects.

4.0 PERFORMANCE EVALUATION

The performance evaluation required fabricating the airfoils, testing the cascade in a transonic tunnel, and analyzing the test data to determine the extent to which the design objectives were met.

4.1 Cascade Airfoil Fabrication

Ten cascade airfoils of 69.85 mm (2.75 in.) chord and 167.64 mm (6.6 in.) span were manufactured from a steel alloy. Surface contour tolerances of $\pm$0.05 mm ($\pm$0.002 in.) were specified and contour inspections made with a New England Airfoil Tracing Machine at three span locations on each airfoil. All ten airfoils were well within specified tolerances. Three airfoils were selected for static pressure instrumentation on the basis of this inspection. A total of seven airfoils were selected for installation in the cascade tunnel.

4.2 Description of Test Facility

The transonic cascade facility used in this investigation was built by NACA-Langley in the early 1950's and transferred to the DFVLR (Deutsche Forschung and Versuchsanstalt fur Luft and Raumfahrt) in Porz-Wahn, West Germany in 1963 (14). This facility was used to test

14. Starken, H., Breugelmans, F. A. E., and Schimming, P., "Investigation of the Axial Velocity Density Ratio in a High Turning Cascade," ASME Paper 75-GT-25, ASME Gas Turbine Conference and Products Show, Houston, Texas, March 1975.

the original Korn supercritical cascade design. Figure 6 shows the cascade test section as it is currently installed at the DFVLR. A schematic cross-section to the test section is shown in Figure 7.

4.2.1 Tunnel Operating Conditions and Operation

The transonic cascade tunnel is a closed loop, continuously running facility with variable nozzle and variable test section height. This tunnel is unique in its extensive endwall boundary layer control system and in its substantial vacuum capacity, capable of removing as much as 50 percent of the total tunnel flow through various bleed systems. These provisions are essential for controlling the secondary flows induced by the strong gapwise pressure gradients of the supercritical cascade. The dry air is delivered by a set of compressors with a total installed power of 5000 KW (3728 Hp) and a mass flow of up to 20 kg/sec (44 lbm/sec). The tunnel test section height is variable between 150 mm (5.9 in.) and 450 mm (17.7 in.), and the span is 167 mm (6.6 in.). These dimensions yield an aspect ratio of 2.4 for a airfoil chord of 69.85 mm (2.75 in.). The tunnel Reynolds number can be varied from 4×10^5 to 4×10^6 by changing the settling chamber pressure. The nozzle is half-symmetrical with a variable shape adjustment for the upper half and a variable height adjustment for the flat lower half. This arrangement provides an inlet Mach number range from 0.0 to 1.4. The inlet Mach number is uniform over the test section height within $\pm$1.5 percent of the maximum, and the turbulence level in the inlet is 0.5 ($\pm$0.2) percent for an inlet Mach number of 0.3 to 0.7.

The upper wall of the test section is slotted and equipped with suction to improve the inlet flow conditions. Additional suction capability is available for boundary layer removal ahead of the test section (slots in the sidewalls reaching from the nozzle top to the bottom wall) and through chordwise slotted cascade endwalls within the airfoil pack. The tunnel top endwall flow is separated from the cascade core flow by a tailboard system hinged at the trailing edge of the outermost cascade airfoil. The tunnel bottom endwall flow is controlled by a movable endwall flap. A lower tailboard is not used.

4.2.2 Instrumentation

The inlet and exit static pressure was measured by static taps on the cascade wall. For this cascade, the upstream measurement plane was axially 25 mm (0.984 in.) from the leading edge plane. The exit measurement plane was 22 mm (0.866 in.) from the trailing edge plane. The inlet air angle was measured at the same gapwise locations for three consecutive airfoil channels. The downstream traverse probe measured a combination of pressures, providing both total and static pressures as well as flow angle for the complete wake traverse information. The traverse system was operated in a stepping mode during loss measurements to ensure sufficient time for the

probe-transducer system to accurately measure the total pressure, static pressure, and flow angle in portions of the wake with strong flow gradients.

The cascade airfoils were heavily instrumented with surface pressure taps. The airfoil thickness required the instrumentation of three separate airfoils rather than just one. One airfoil was pressure tapped chordwise on the suction surface, a second on the pressure surface, and a third was instrumented spanwise on both surfaces at only a few chordwise locations. The pressure and suction instrumented airfoils were arranged in cascade to record the flow within a common passage.

4.3 Testing Procedure and Data Acquisition/Reduction

The demonstration of the accuracy of the supercritical design system through comparisons with measured cascade data required precise control of the experimental setup to ensure that the desired aerodynamic conditions were closely matched. The testing procedure and data acquisition necessary to achieve the required accuracy are described in Sections 4.3.1 and 4.3.2.

4.3.1 Testing Procedures

The inlet angle of the cascade relative to the inlet duct was set to produce the correct inlet flow angle (angle accuracy of 0.5 degree or less is possible). The inlet Mach number was then set at the desired value, and, to ensure that the measured performance was obtained under periodic flow conditions, several procedures were followed. Tunnel periodicity was checked by comparing the inlet flow angle as measured at three adjacent gap positions and by observing the inlet and exit static pressure distributions displayed on manometer boards located in the test cell control room. The exit traversing probe was operated in a continuously running mode, enabling three adjacent blades to be traversed in a reasonable length of time. The resulting wake profiles were displayed on a plotter to check airfoil wake shape consistency. In addition, wake traverses at various spanwise locations were measured to guarantee that an acceptable portion of the airfoil was operating under two-dimensional conditions. Adjustments to obtain periodic flow conditions were then performed on the movable bottom endwall, flap, upper tailboard, and on the extensive boundary layer control vacuum system. Further adjustments in upstream pressure were also required to maintain the desired inlet Mach number.

4.3.2 Data Acquisition/Reduction

The complete information for each test point was recorded by a computer-controlled automatic data acquisition system and stored on magnetic tape. This information included plenum conditions, inlet static pressures, inlet flow angles, airfoil surface pressure distributions, and downstream wake traverse data.

An on-line data reduction system provided an immediate summary of computed performance information, which was displayed on a computer terminal located in the test cell control room. The airfoil design surface Mach number distribution was also graphically compared with the measured distribution, permitting an evaluation of the test point results.

A complete off-line data reduction system provided detailed test information, including corrections for probe calibrations. The cascade total pressure losses were computed from the wake data using a control volume mixing analysis.

4.4 Test Results

The cascade performance was measured at test conditions best matching the design surface Mach number distribution. Test conditions were also systematically varied over a wide range of inlet flow angles and inlet Mach numbers to determine the off-design performance. Complete test data points were acquired at 79 conditions. Thirty-seven of these test data points, judged to have the most periodic cascade flow, were used in the final performance evaluation. A summary of the reduced data for these 37 points is presented in the data table in the Appendix.

The best experimental match of the design surface Mach number distribution is shown in Figure 8. This match was obtained at the design inlet angle and an upstream Mach number 0.03 lower than expected. This slight difference most probably resulted from tunnel sidewall boundary layer growth upstream of the leading edge plane of the cascade. The design calculation was performed assuming a linear distribution of stream tube contraction between the cascade leading edge and downstream measurement planes. An upstream Mach number of 0.73 (measured in the tunnel test) results in an average leading edge Mach number of 0.[illegible] (design), if a roughly 1.6 percent stream tube contraction is assumed to occur between these two locations. This is not an unreasonable amount of area change, despite the incorporation of upstream boundary layer removal slots in the tunnel sidewalls. Numerical simulations of near design test point 72, combining the transonic and boundary layer analyses, further substantiated this interpretation of the results. These simulations are discussed in Section 5.0. At the test design point, the experimental surface Mach number distribution closely matched that of the design. The suction surface appeared to be shock free and analysis of the boundary layer indicated that it remained attached through its diffusion. The measured turning was within one degree of the design value. The measured total pressure loss, expressed as a fraction of the inlet compressible dynamic head, was 0.02. Thus the design requirements were met for turning, loss, and surface Mach number distribution.

The total pressure loss characteristics obtained with varying the inlet Mach numbers at the design flow angle are shown in Figure 9. The loss

is nearly constant at 0.02 up to the design point (M upstream = 0.73, M leading edge = 0.76). At a Mach number 0.03 greater than the design point, the loss doubles to a value of 0.04. This Mach number range is adequate for this application, since this fan stator mean section has an inlet Mach number of 0.8 or less throughout its operating range.

Loss data for off-design inlet flow angles with varying inlet Mach numbers are shown in Figures 10 through 15. These inlet angles correspond to incidence angles of +7, +5, +3, -3, -5, and -10 degrees. These data shown in Figure 16, fully define the useful operating range of the cascade. The measured upstream Mach number has been used on all of these figures. As in the case of the design point, numerical simulations of off-design conditions suggest that average Mach numbers for the upstream and leading edge are slightly different. Test and design values, then, should be carefully related if precise comparisons are required. At various angles of incidence, numerical simulations were made for test conditions having both low total pressure losses and high inlet Mach numbers. The simulations indicated that the Mach number increase of 0.03 gave the most satisfactory result. Thus, the loss bucket for the design Mach number of 0.76 would be an interpolated line on Figure 16 at an inlet Mach number of 0.73. A significant range of positive and negative incidence around the design inlet angle is present before losses increase to prohibitive levels.

Figure 17 depicts flow turning and exit flow angle versus inlet flow angle. Exit flow angle was nearly constant, ranging from approximately 89 to 91 degrees. This nearly constant exit angle over all test conditions is a significant accomplishment of this airfoil design. This air exit angle consistency is particularly important for the bypass portion of the fan stators, which must turn the flow to an axial discharge angle to maximize fan duct thrust.

The test results indicate that the supercritical airfoil has met its design requirements and has operated efficiently over a wide range of aerodynamic conditions. The test data taken at the design point conditions indicate (1) a good match between measured and design surface Mach number distributions, (2) an attached suction side boundary layer resulting in low loss, and (3) an exit angle within one degree of design specifications. These results indicate that the shockless flow field, combined with firm control of the suction surface diffusion rate, results in an attached boundary layer essential to good aerodynamic performance. In conclusion, these results demonstrate the validity of this design method for future design work.

5.0 ANALYTICAL SIMULATIONS

Analytical simulation of the near design test condition, as well as several off-design conditions, has been carried out. These conditions are test points 72, 02, 60, 42, 47, 32, and 38 shown in Figures 9 through 15. The simulation procedure is the same as that used in previous analysis work and has been described in detail by Stephens (7). This procedure is comprised of the transonic cascade analysis, an integral boundary layer calculation, and a simple wake unmixing calculation. These simulations provide valuable insight into the operation of the tunnel. They are also an excellent check on the validity of the design system, since the analysis and design methods are closely related. Results for the design point and a negative 10 degree incidence point are shown in Figures 18 and 19.

In setting up an analytical simulation of the test conditions, it was necessary to account for the stream tube contraction caused by tunnel sidewall boundary layer growth upstream of the cascade leading edge. The tunnel contraction affects the total velocity vector. The best means of simulating this contraction is to impose a higher inlet Mach number upstream of the cascade leading edge. The Mach number increase used was 0.03, corresponding to a one-dimensional area contraction of 1.6 percent. This was found to provide adequate simulation over a wide range of operating conditions, including incidence angles from +5 to -3 degrees. The results of the design point simulation, including boundary layer and laminar bubble effects, predicted via Roberts' (15) method, are shown in Figure 18. The agreement shown between the calculations and the experiment is quite good.

At more severe negative incidences, such as -10 degrees, the best simulation was achieved by using a -1.2 percent upstream stream tube contraction while retaining a linear distribution of stream tube contraction through the cascade. This result is shown in Figure 19. If only agreement at the leading edge were required, the Mach number increase of 0.03 would have provided an adequate match; however, a nonlinear stream tube contraction distribution would be required to match the remainder of the airfoil.

The full explanation of this tunnel phenomena is beyond the scope of the contract work. There are undoubtedly other tunnel effects, such as the relative amounts of sidewall suction used in the upstream boundary layer removal slots and in the cascade passage sidewall slots, which would influence the upstream boundary layer growth. Consideration is included here mainly because the effect, if left unexplored, would have obscured the observations of the excellent comparisons between the test and design surface Mach number distributions.

---

15. Roberts, W. B., "The Effect of Reynolds Number and Laminar Separation on Axial Cascade Performance," ASME Paper 74-GT-68, March 1974.

6.0 CONCLUSIONS

1. A procedure developed at Pratt & Whitney Aircraft has been used to design a supercritical cascade to satisfy practical requirements.

2. The cascade operated with low total pressure loss at the design point and achieved the required flow turning within less than one degree.

3. The design surface Mach number distribution was closely matched in the test. The airfoil appeared to be shock-free and the suction side boundary layer remained attached throughout its diffusion to the trailing edge.

4. Off-design performance in terms of Mach number range, incidence range, and flow turning was very good over a broad range of operating conditions.

5. The flow exit angle was maintained to within ± 1 degree of design (axial) for upstream Mach numbers ranging from 0.4 to 0.75 and over a range of inlet incidence angles from -10 to +7 degrees.

6. The loss rise characteristics at the design inlet flow angle were successfully controlled to provide a 0.03 margin in inlet Mach number before the measured loss doubled.

7. An analytical simulation of the test design point conditions provided excellent agreement between computed and measured surface Mach number distributions.

8. Analytical simulation of a wide variety of off-design test conditions further substantiates the accuracy of the flow modelling procedure for supercritical transonic flows.

9. Analytical simulations suggest that an approximate increase in average Mach number of 0.03 exists between the upstream measuring plane and the airfoil leading edge plane. It is probable that this effect in the DFVLR tunnel is caused by sidewall boundary layer growth, which reduces the duct area by about 1.6 percent between these planes for this cascade.

(a) $M_1 = 0.625$ (b) $M_1 = 0.671$

(c) $M_1 = 0.702$ (d) $M_1 = 0.717$

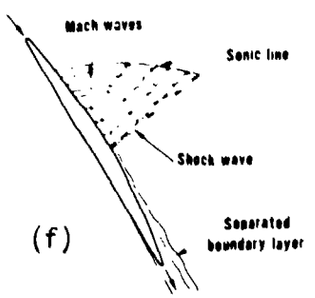

(f)

Figure 1 (a-e) Schlieren Photographs Showing Cascade Flow Field for a Range of Increasing Inlet Mach Numbers (see Reference 1). (f) Schematic of the High-Loss Condition shown in (e)

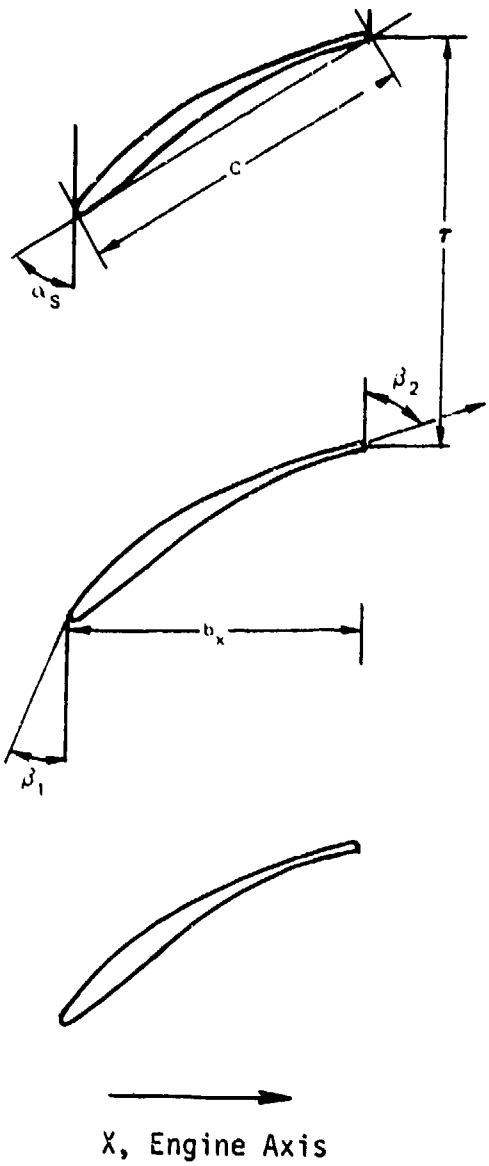

GEOMETRIC DATA

C = 2.80 in.
r/C = 1.195
α_s = 58 DEGREES
b_x = 2.37 in.

AERODYNAMIC DATA

M_1 = 0.78
M_2 = 0.48
β_1 = 43.0 DEGREES
β_2 = 68.0 DEGREES
TURNING = 25.0 DEGREES
AVDR = 1.03

Figure 2 Korn Supercritical Cascade Geometry and Aerodynamic Data

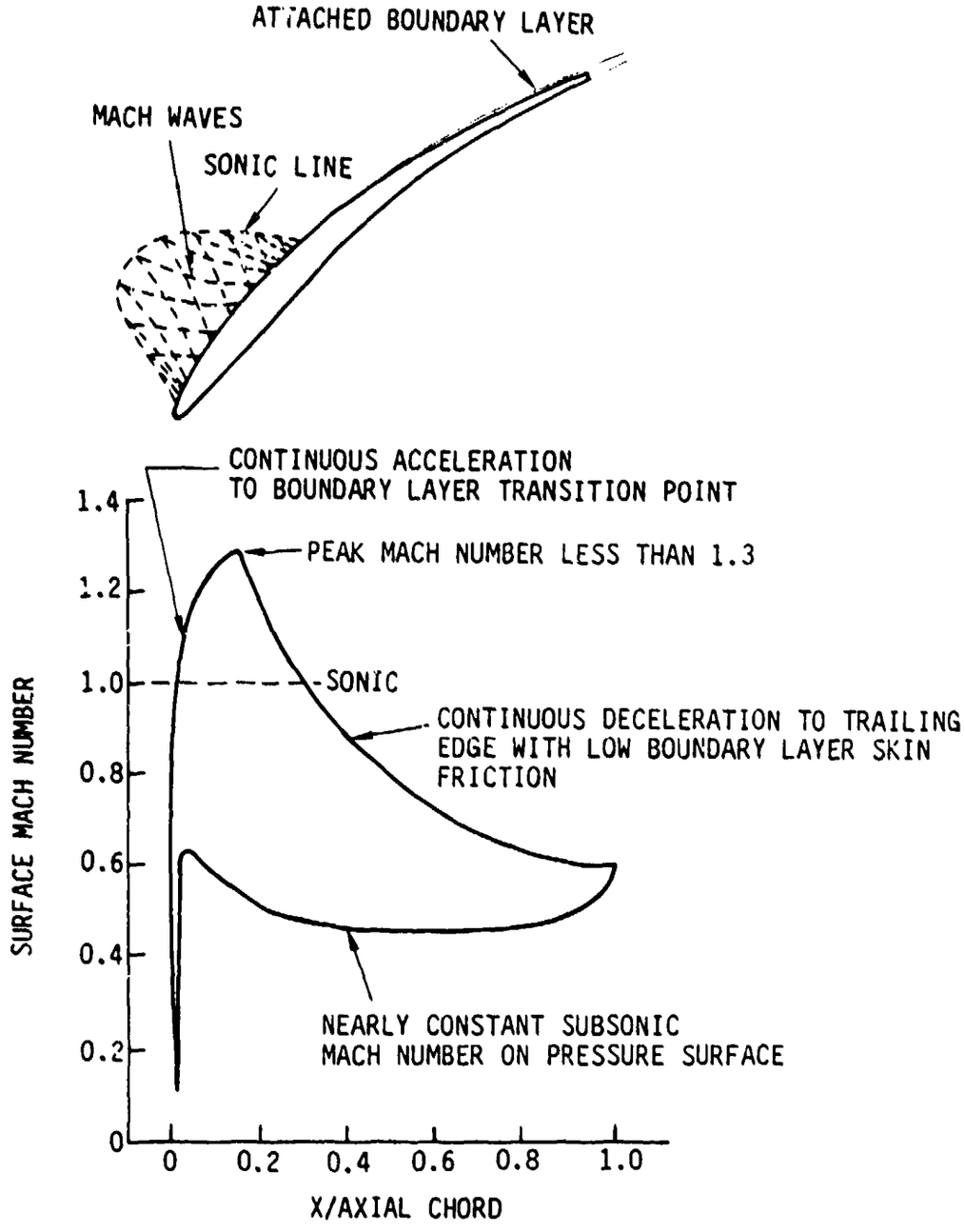

Figure 3 Supercritical Airfoil Aerodynamic Design Requirements

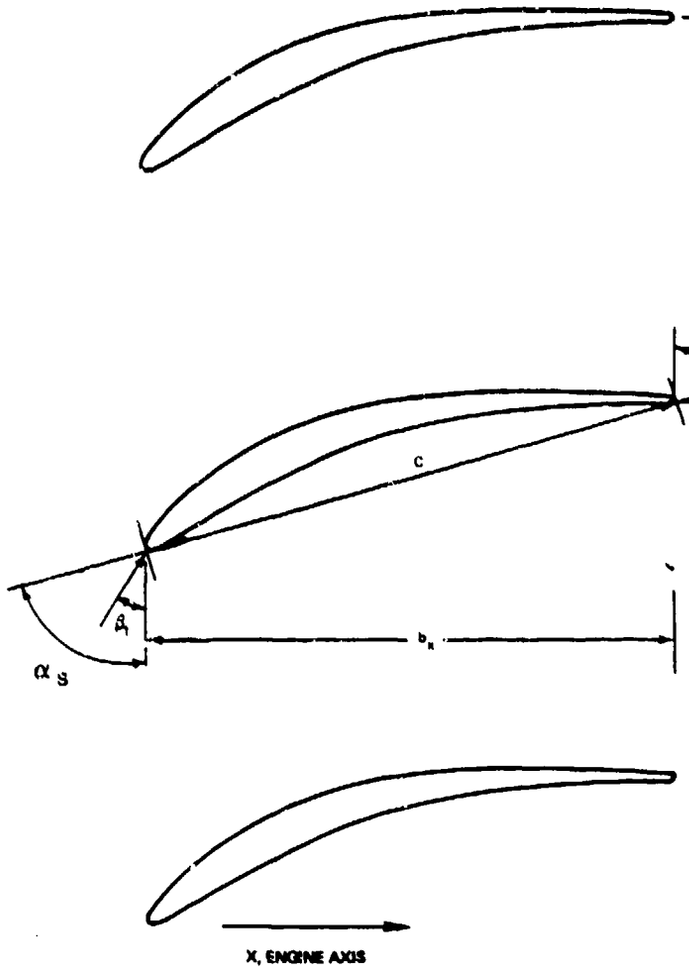

GEOMETRIC DATA

C = 2.75 in.
τ/C = 0.70
α_S = 74.25 DEGREES
b_X = 2.65 in.

AERODYNAMIC DATA

M_1 = 0.763
M_2 = 0.529
β_1 = 46.8 DEGREES
β_2 = 90.0 DEGREES
TURNING = 43.2 DEGREES
AVDR = 1.124

Figure 4 Supercritical Cascade Geometry and Aerodynamic Design Conditions

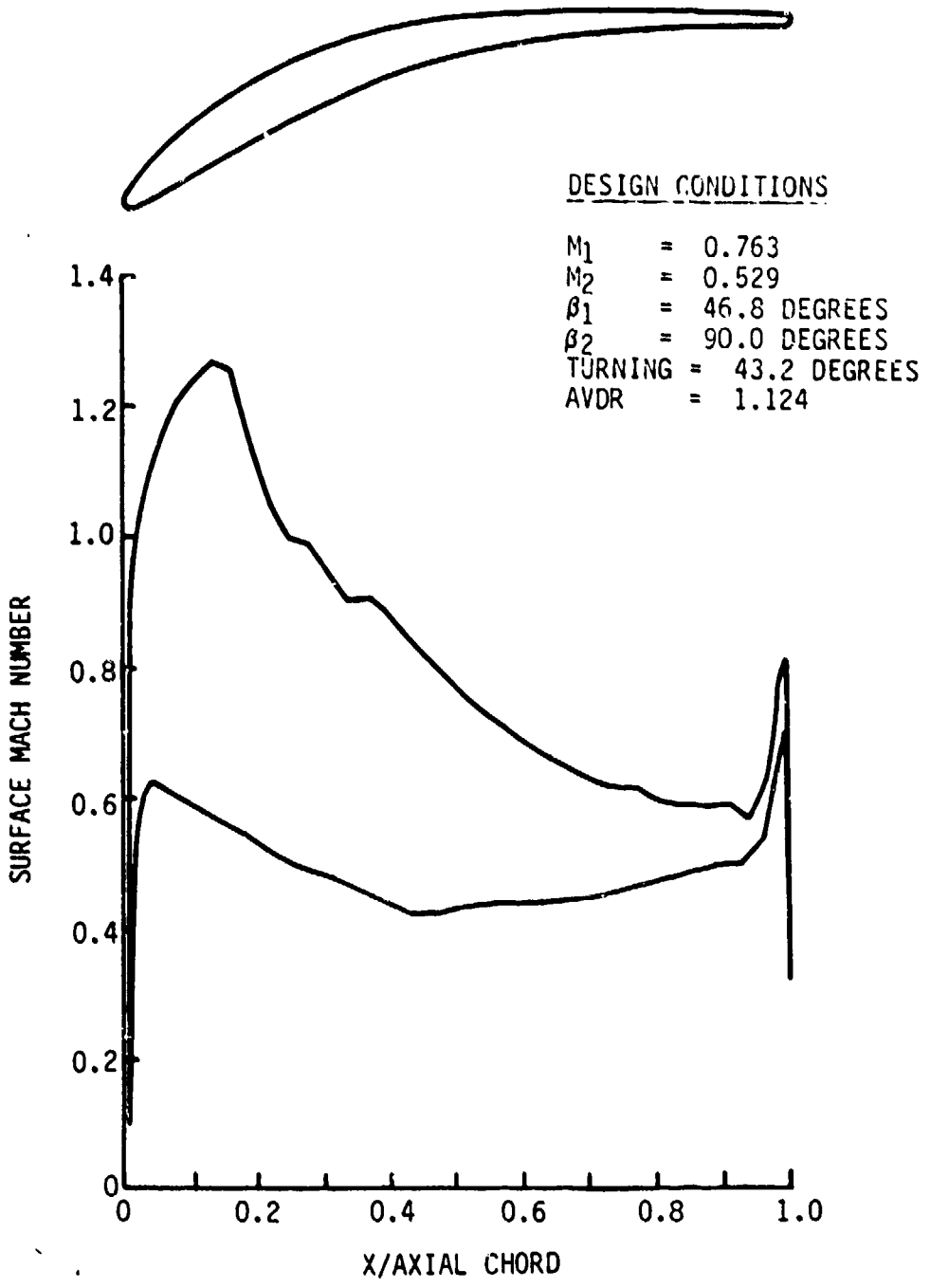

Figure 5 Supercritical Cascade Design Surface Mach Number Distribution

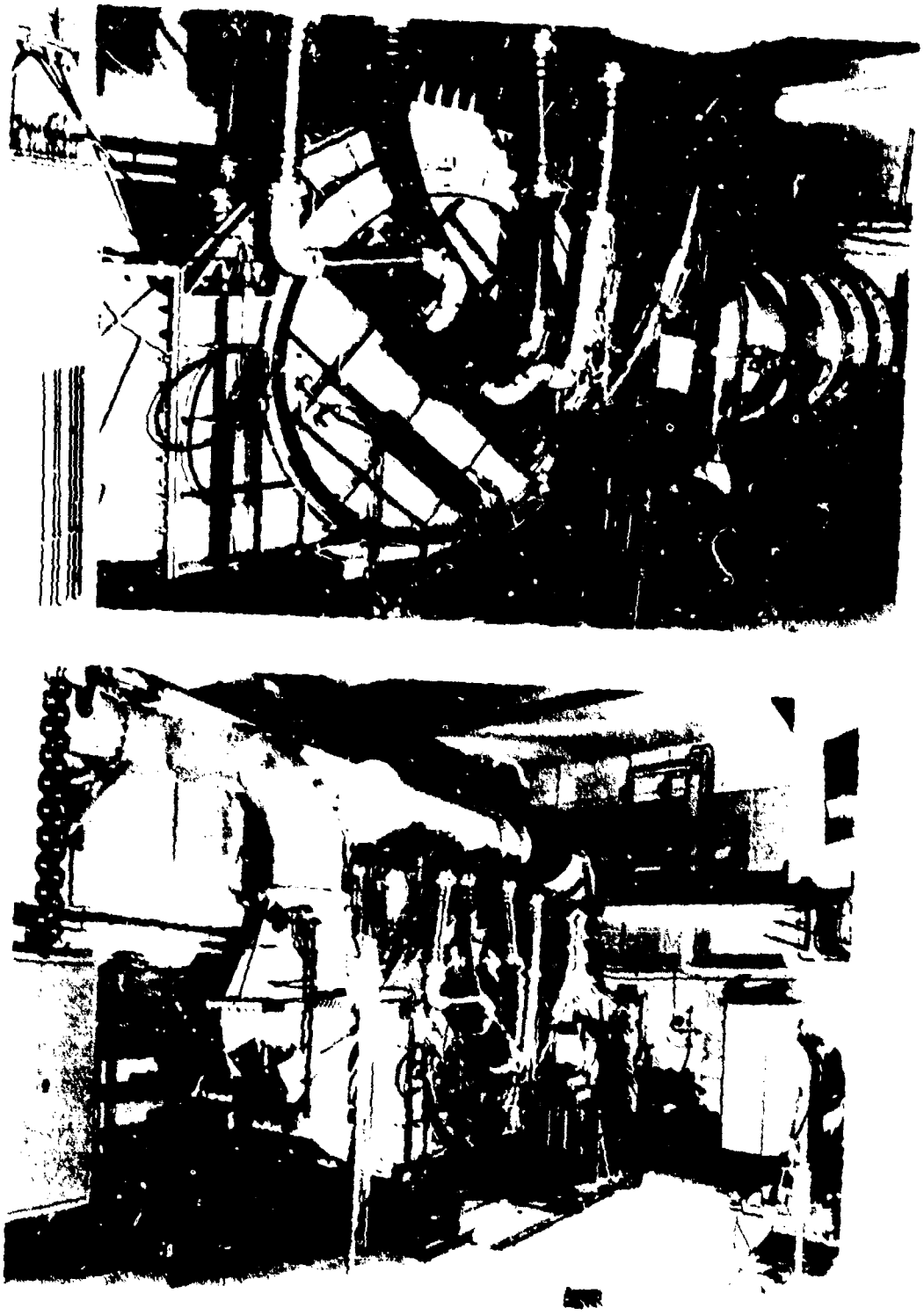

Figure 6 DFVLR Transonic Cascade Test Facility

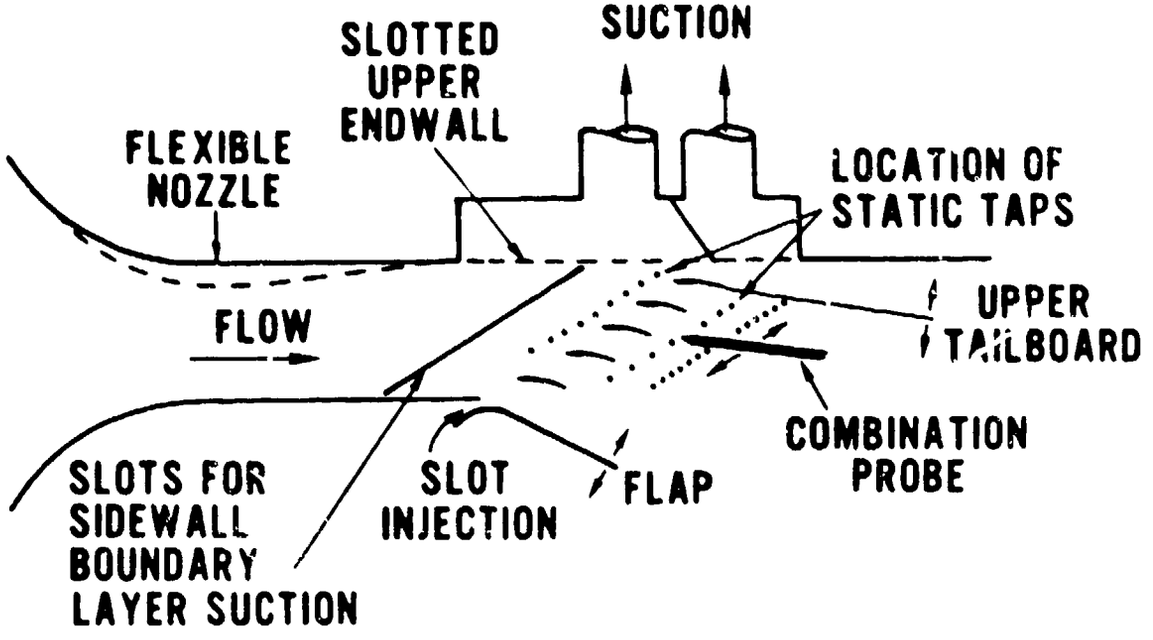

Figure 7 Schematic of DFVLR Transonic Cascade Test Section

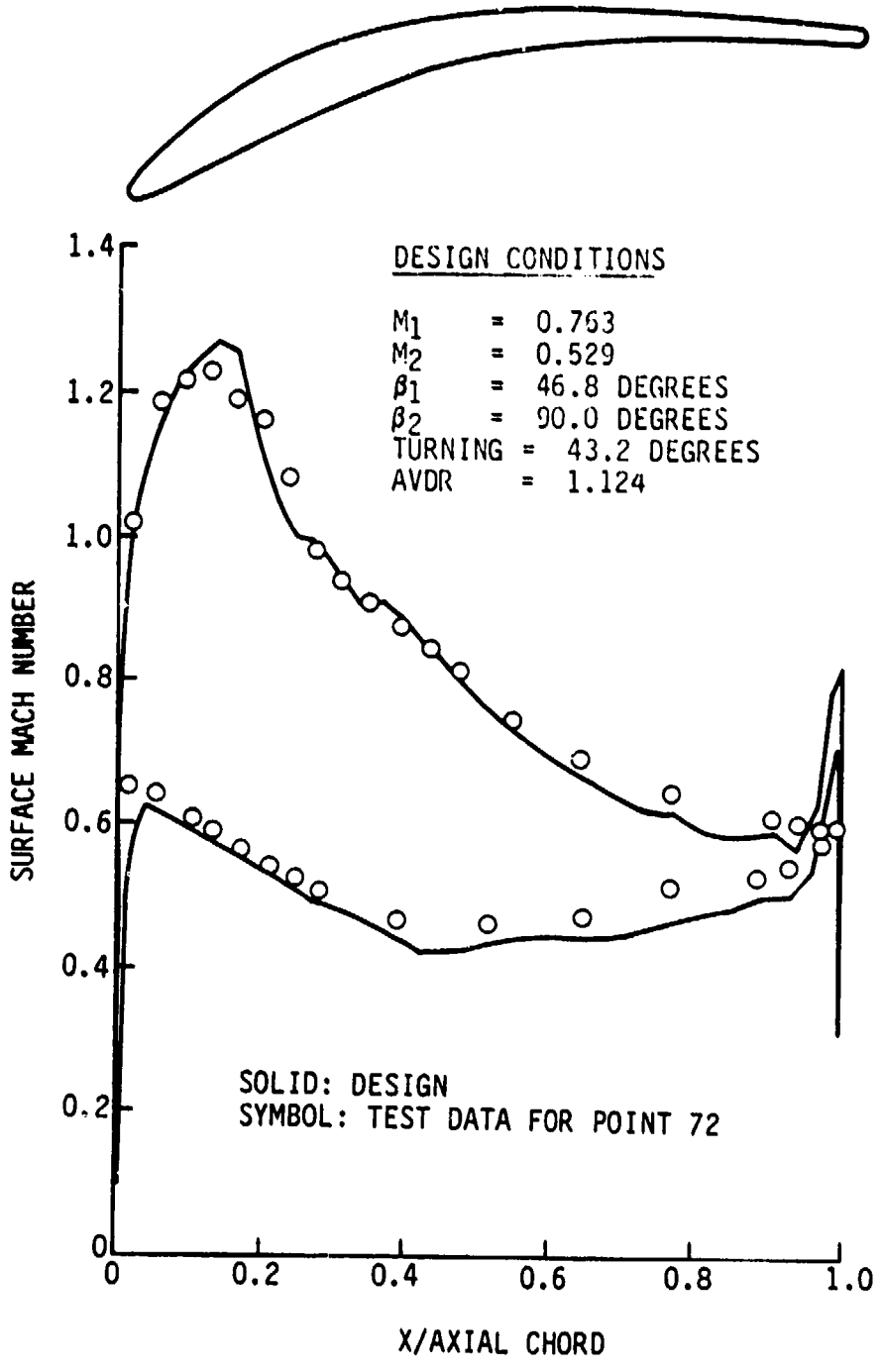

Figure 8 Comparison of Design Mach Number Distribution and the Measured Test Data.

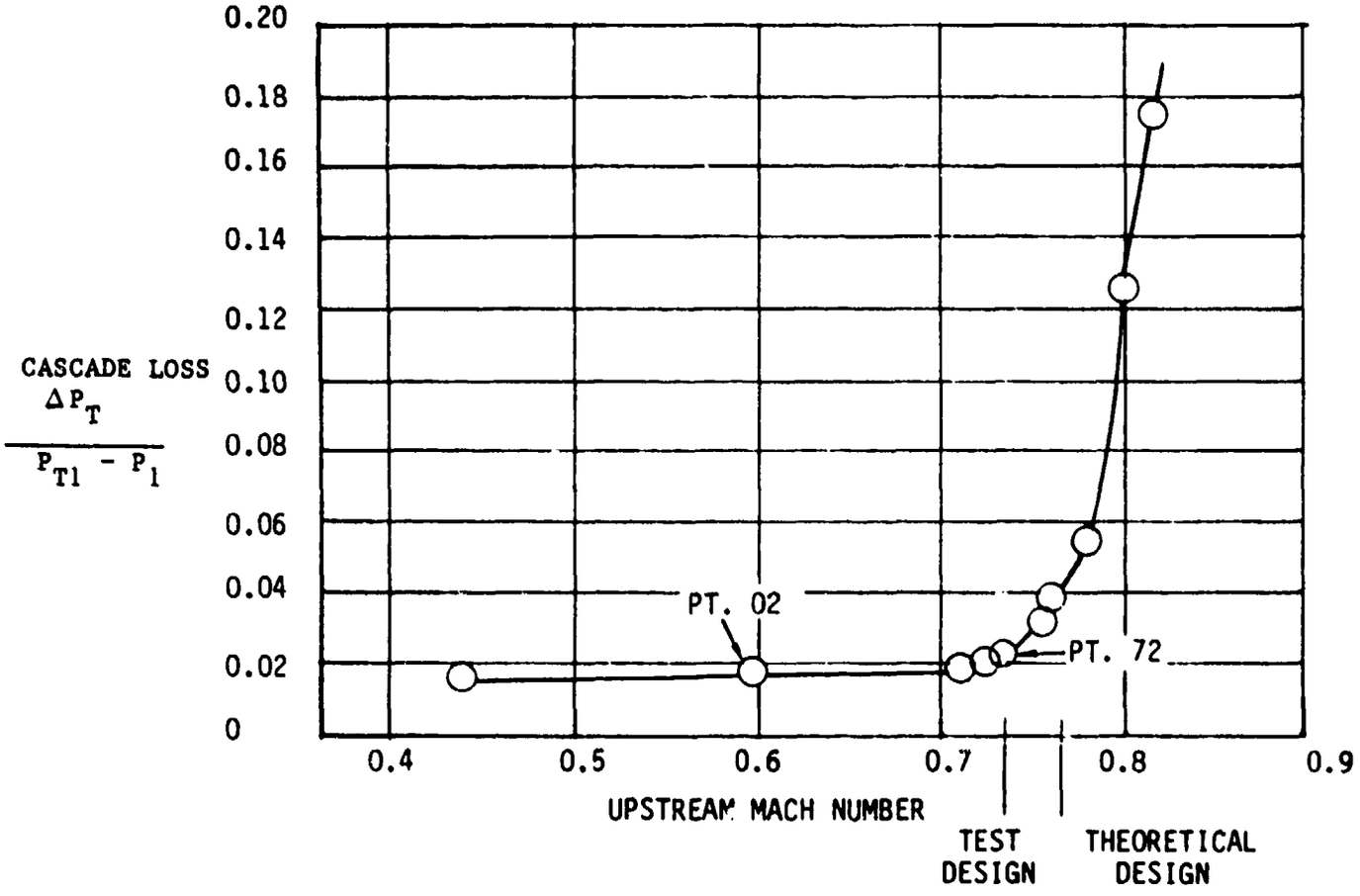

Figure 9 Cascade Performance - Loss versus inlet Mach number at design inlet angle.

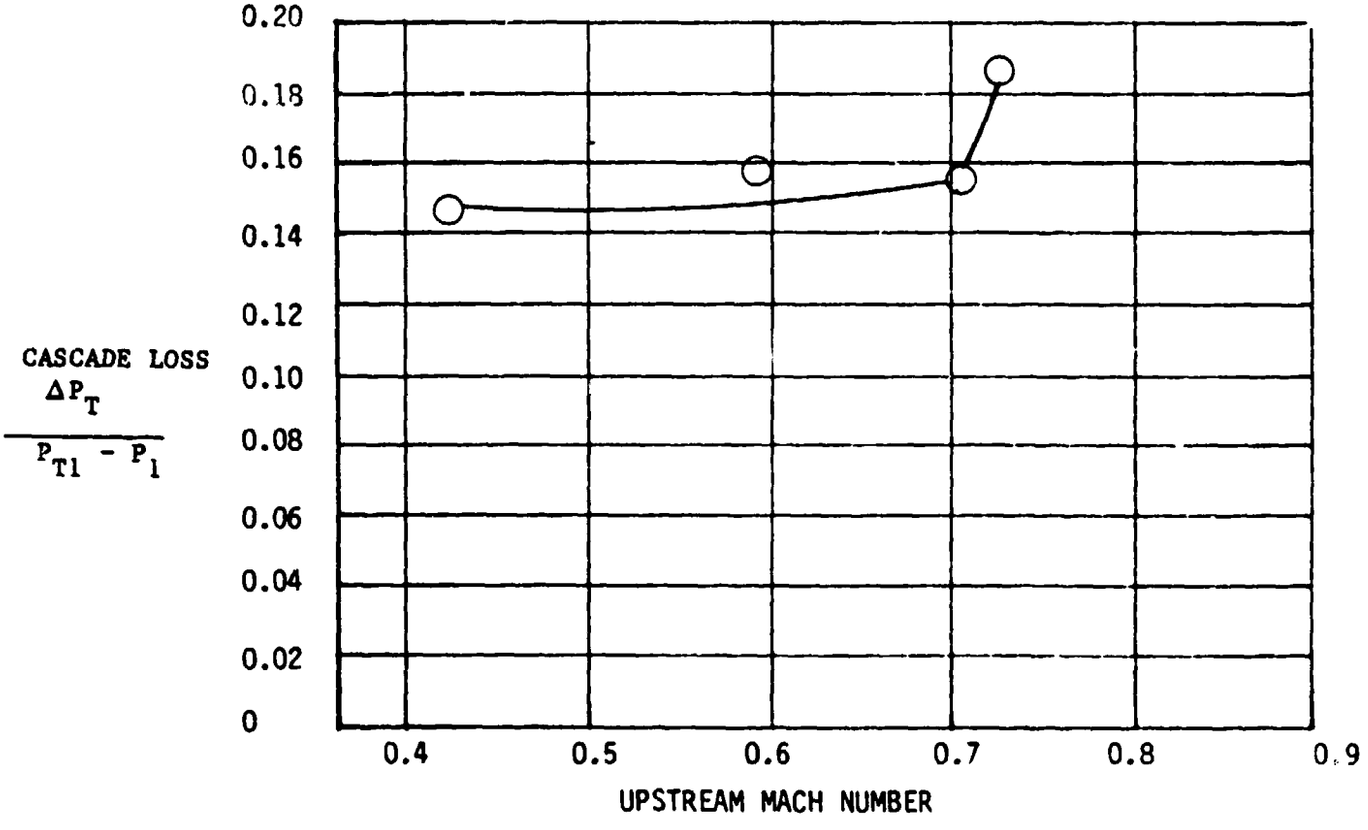

Figure 10 Cascade Performance - Loss versus inlet Mach number at +7 degrees incidence.

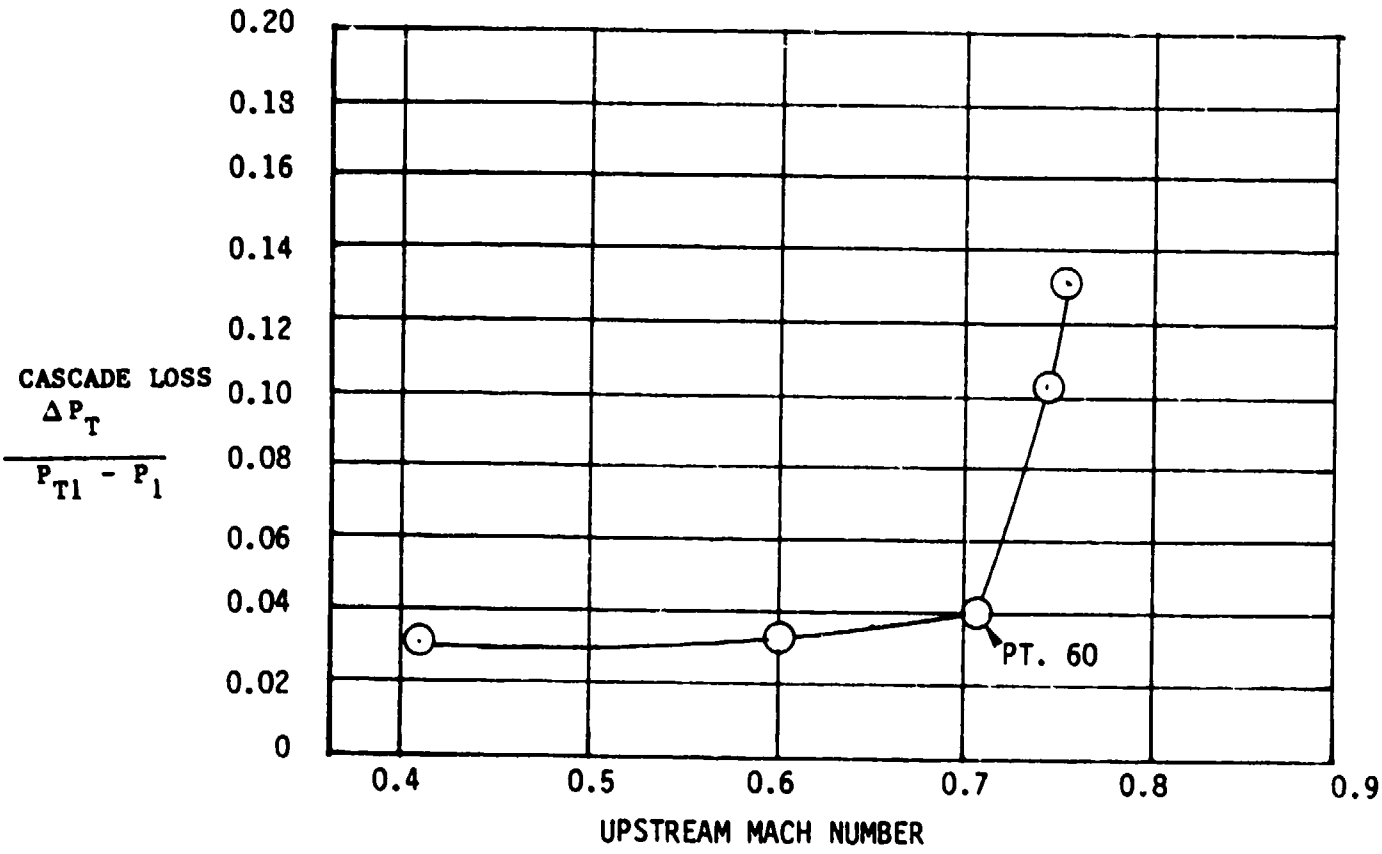

Figure 11 Cascade Performance - Loss versus inlet Mach number at +5 degrees incidence.

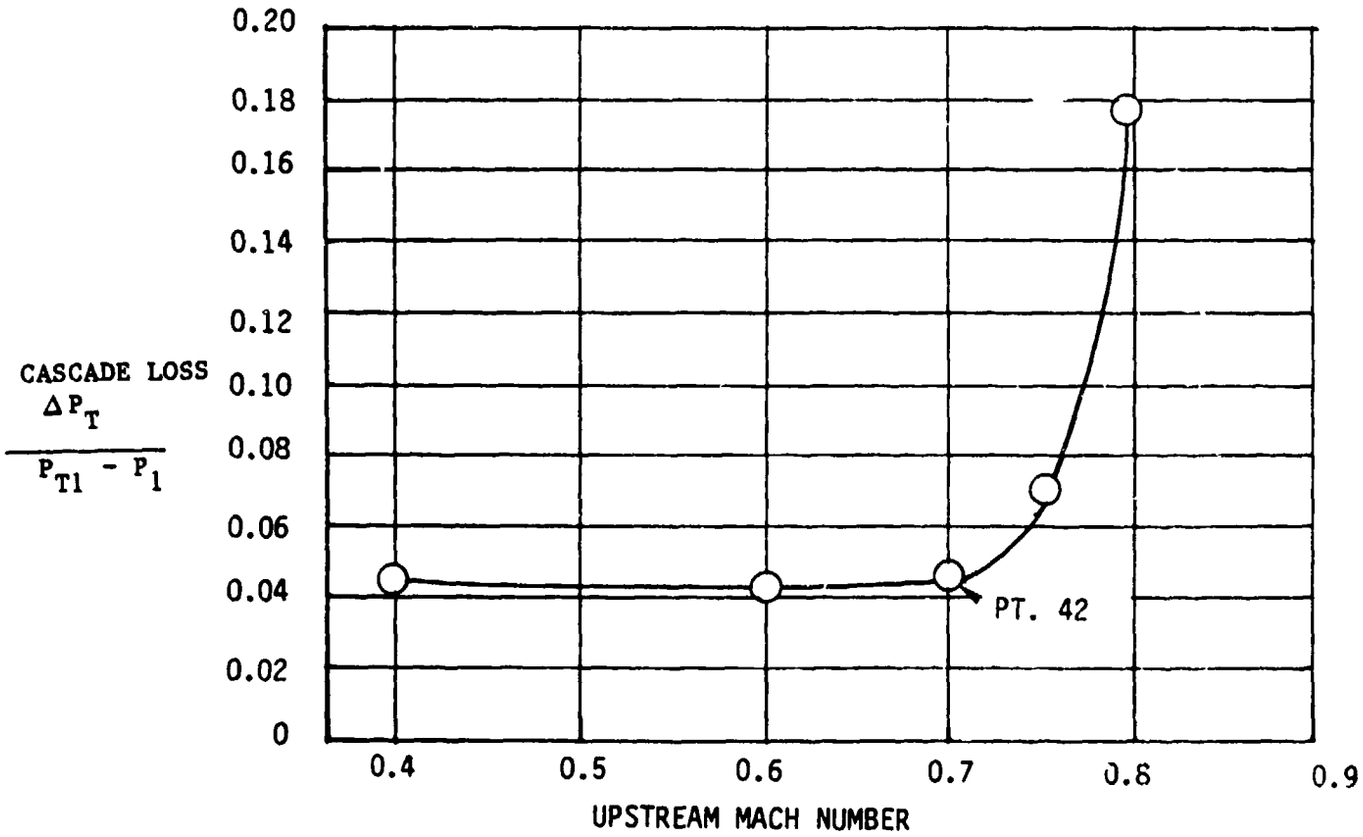

Figure 12 Cascade Performance - Loss versus inlet Mach number at +3 degrees incidence.

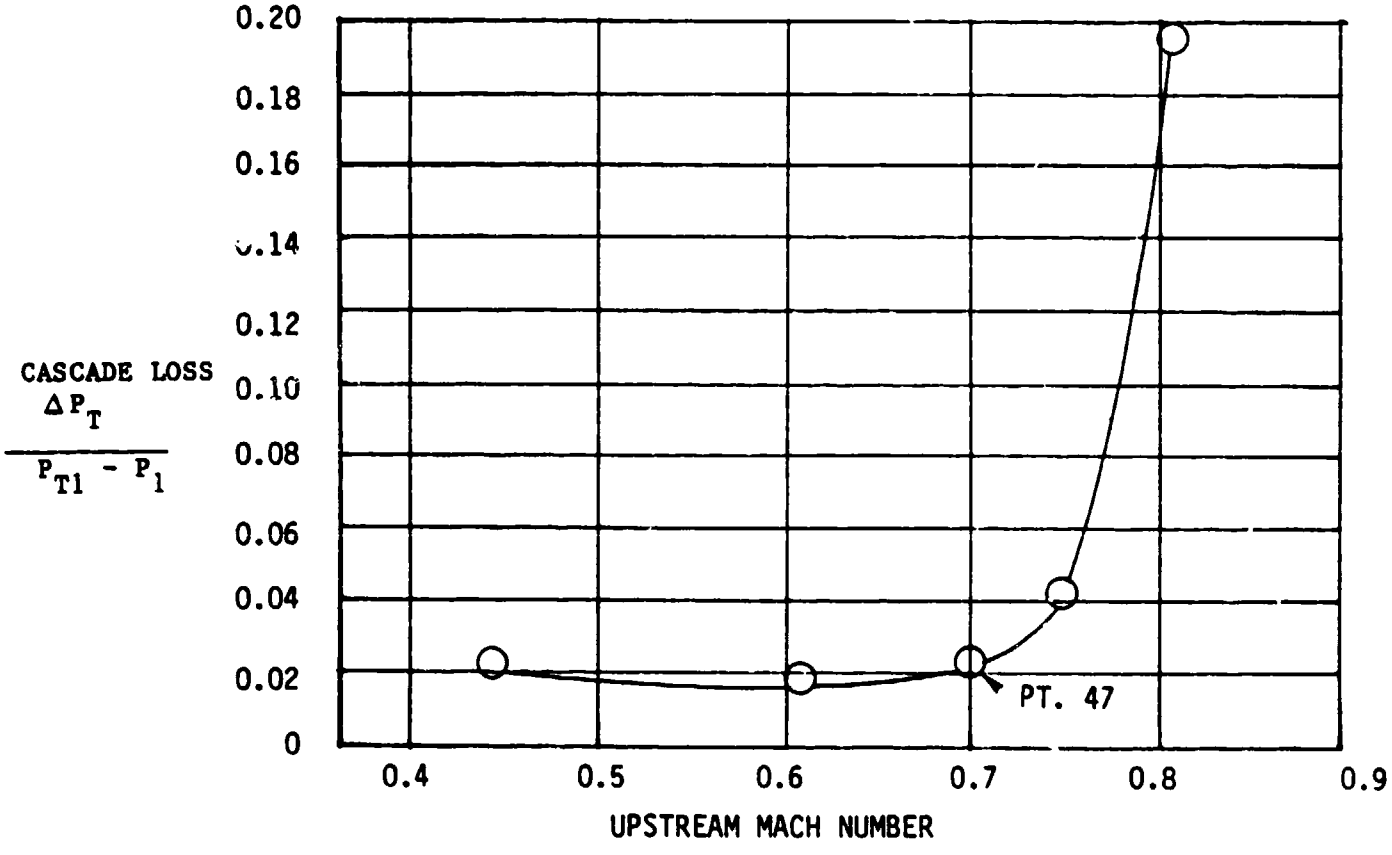

Figure 13 Cascade Performance - Loss versus inlet Mach number at -3 degrees incidence.

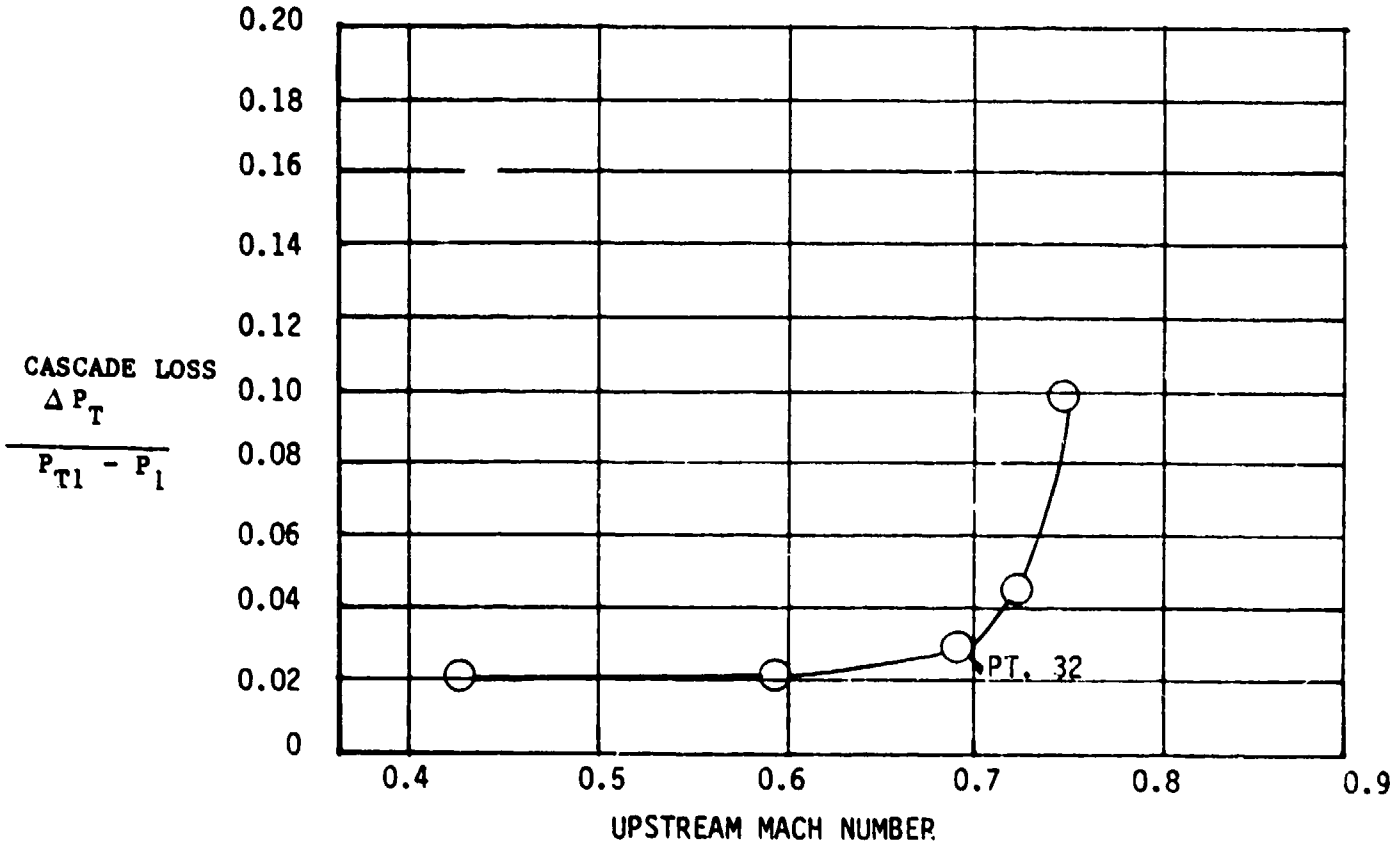

Figure 14 Cascade Performance - Loss versus inlet Mach number at -5 degrees incidence.

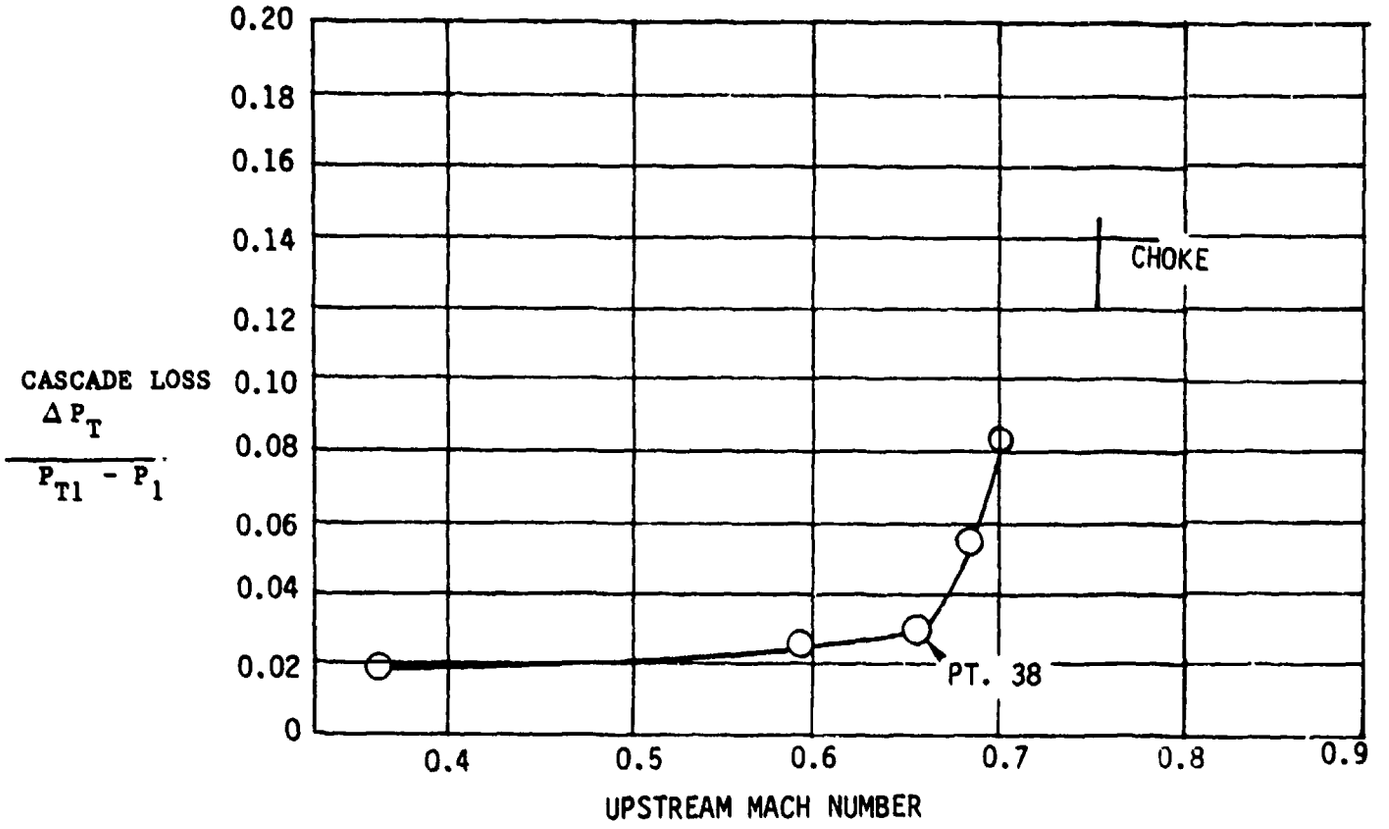

Figure 15 Cascade Performance - Loss versus inlet Mach number at -10 degrees incidence.

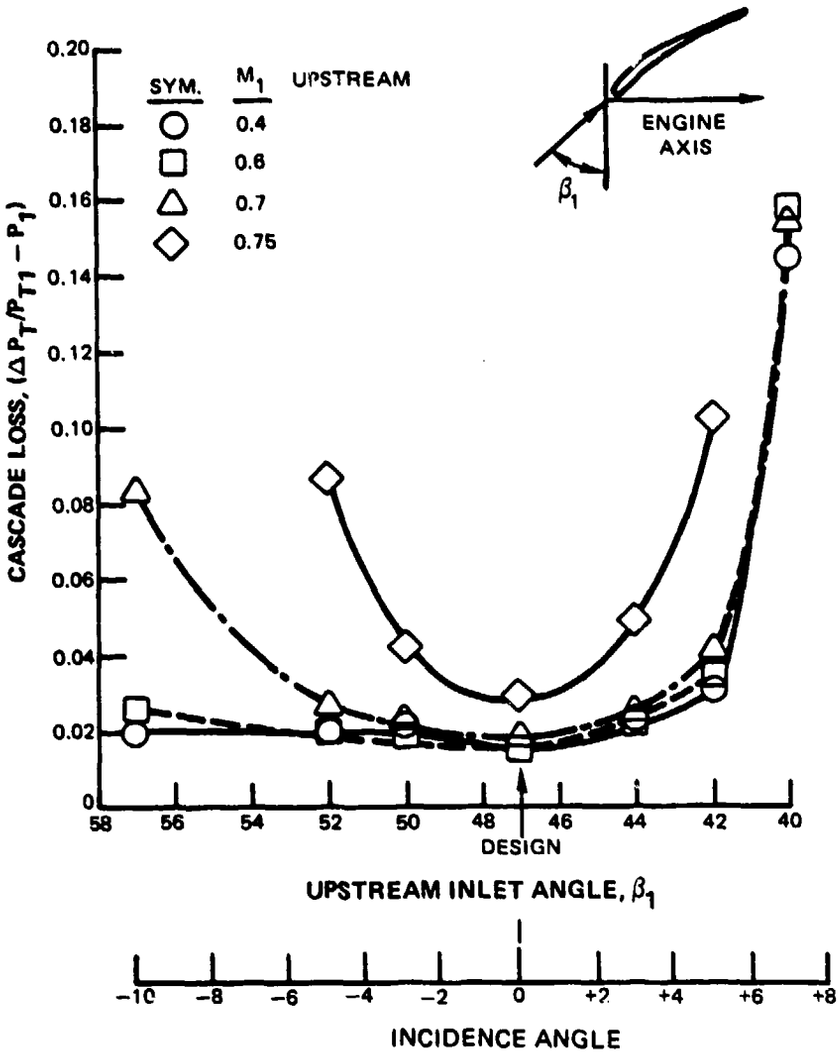

Figure 16 Cascade Performance - Loss as a function of cascade inlet angle or incidence for various upstream Mach numbers.

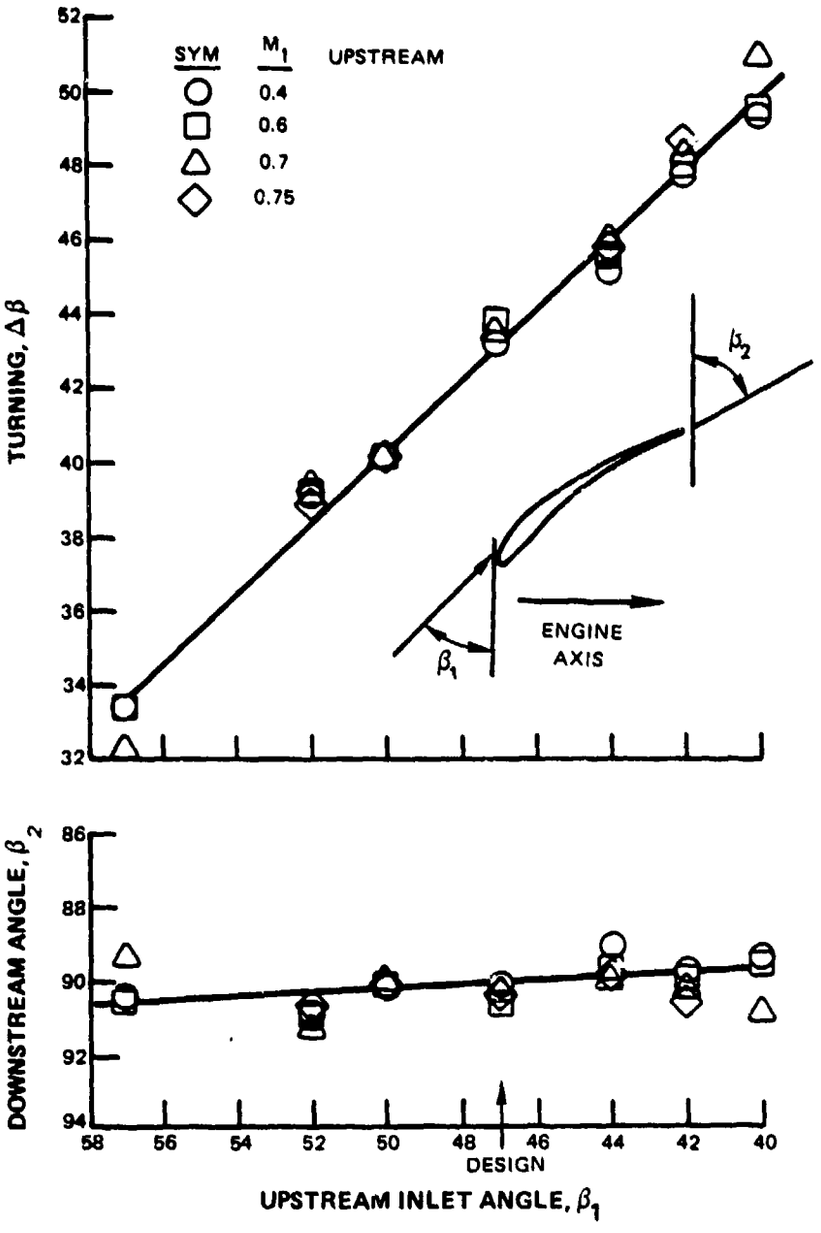

Figure 17 Cascade Performance - Flow turning and exit flow angle as a function of inlet angle for various upstream Mach numbers.

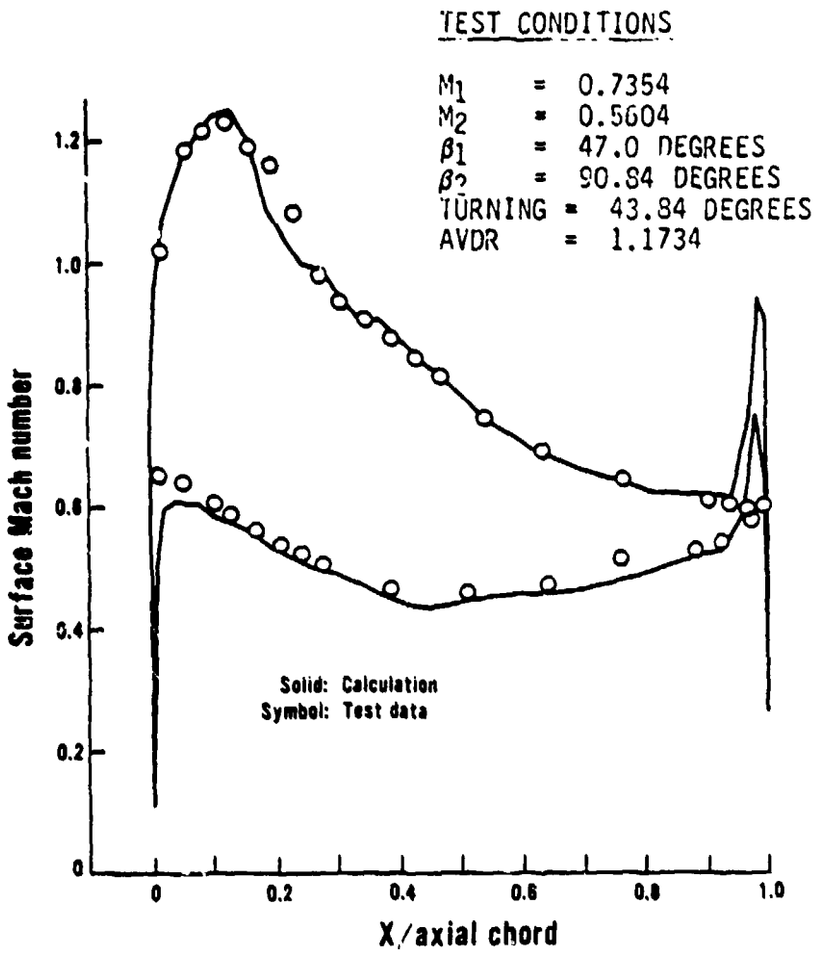

Figure 18 Results of Analytical Simulation of Near Design Test Condition (Point 72)

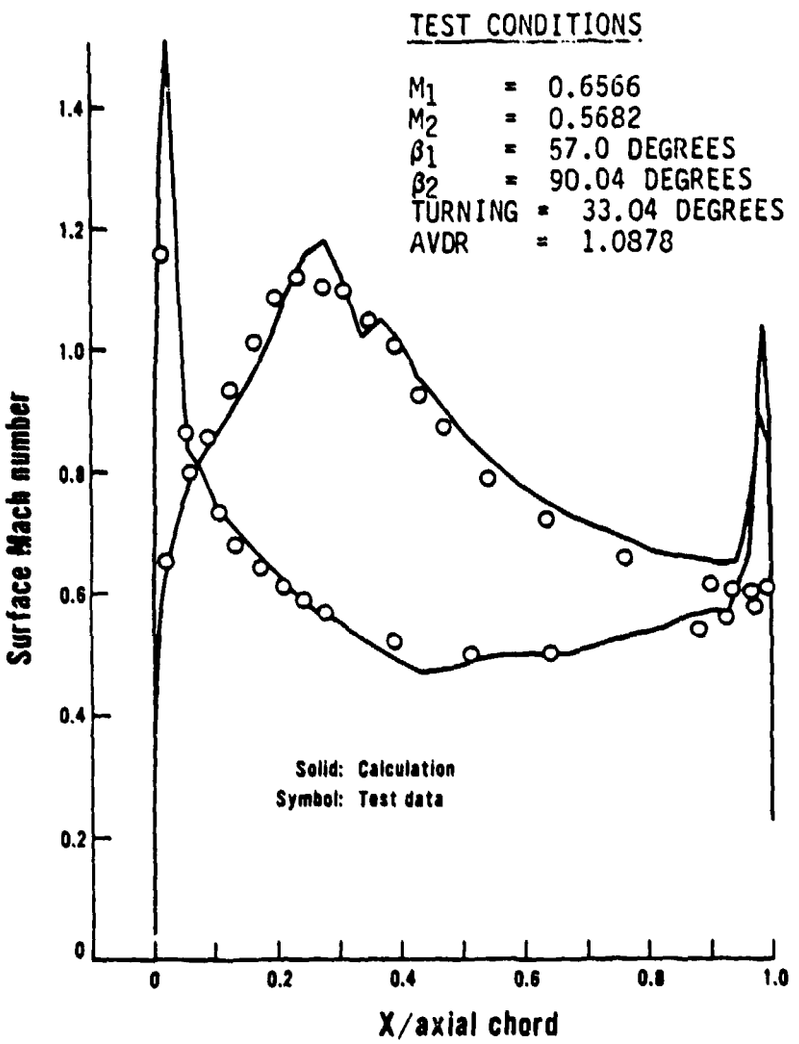

Figure 19 Results of Analytical Simulation of Ten Degree Negative Incidence Test Condition (Point 38)

REFERENCES

1. Dunavant, J. C. et. al. "High Speed Cascade Tests of the NACA 65-($12A_{10}$)10 and NACA 65-(12 A_2I_{8b})10 Compressor Blade Sections," NACA RML55, 108.

2. Whitcomb, Richard T., and Clark, Larry R., "An Airfoil Shape for Efficient Flight at Supercritical Mach Numbers," NASA TMX-1109, May 1965.

3. Bauer, Francis, Garabedian, Paul, and Korn, David, "Supercritical Wing Sections," Lecture Notes in Economics and Mathematical Systems, Vol. 66, Springer - Verlag, New York, 1972.

4. Bauer, Francis, Garabedian, Paul, Korn, David, and Jameson, Antony, "Supercritical Wing Sections II" Lecture Notes in Economics and Mathematical Systems, Vol. 108, Springer - Verlag, 1975.

5. Bauer, Francis, Garabedian, Paul, and Korn, David, "Supercirititical Wing Sections III," Lecture Notes in Economics and Mathematical Systems, Vol. 150, Springer - Verlag, New York, 1977.

6. Korn, David, "Numerical Design of Transonic Cascades," ERDA Research and Development Report COO-3077-72, Courant Inst. Math. Sci., New York Univ., January 1975.

7. Stephens, Harry E., "Application of Supercritical Airfoil Technology to Compressor Cascades: Comparison of Theoretical and Experimental Results," AIAA Paper 78-1138, AIAA Fluid and Plasma Dynamics Conference, Seattle, Wash., July 1978.

8. Ives, David C., and Liutermoza, John F., "Analysis of Transonic Cascade Flow Using Conformal Mapping and Relaxation Techniques," AIAA Journal, Vol. 15, No. 5, May 1977, pp. 647-652.

9. Ives, David C., and Liutermoza, John F., "Second Order Accurate Calculation of Transonic Flow Over Turbomachinery Cascades," AIAA Paper 78-1149, AIAA 11th Fluid and Plasma Dynamics Conference, Seattle, Wash., July 1978.

10. McNally, W. D., "Fortran Program for Calculating Compressible Laminar and Turbulent Boundary Layers in Arbitrary Pressure Gradients," NASA TN D-5681, May 1970.

11. Lieblien, S., and Rouderbush, W. H., "Theoretical Loss Relations for Low Speed Two-Dimensional Cascade Flow," NACA TN 3662, March 1956.

12. Stewart, W. L., "Analysis of Two-Dimensional Compressible Flow Loss Characteristics Downstream of Turbomachine Blade Rows in Terms of Basic Boundary Layer Characteristics," NACA TN 3515, July 1955.

13. Sulam, D.H., M.S. Keenan, and J.T. Flynn, "Single-Stage Evaluation of Highly-Loaded Multiple-Circular-Arc Rotor High-Mach-Number Compressor Stages," NASA CR-7264, PWA-3772.

14. Starken, H., Breugelmans, F. A. E., and Schimming, P., "Investigation of the Axial Velocity Density Ratio in a High Turning Cascade," ASME Paper 75-GT-25, ASME Gas Turbine Conference and Products Show, Houston, Texas, March 1975.

15. Roberts, W. B., "The Effect of Reynolds Number and Laminar Separation on Axial Cascade Performance," ASME Paper 74-GT-68, March 1974.

APPENDIX

NAVAIR SUPERCRITICAL CASCADE DATA SUMMARY

Test Point	M_1	β_1 Design Incidence	R_E	β_2	M_2	Static Pressure Ratio P_2/P_1	Total Pressure Ratio P_{T_2}/P_{T_1}	Flow Turning $\Delta\beta$	$C_P = \frac{P_2 - P_1}{P_{T_1} - P_1}$	$\omega = \frac{P_{T_1} - P_{T_2}}{P_{T_1} - P_1}$	AVDR A_1/A_2	D_F
01	0.4403	46.8	6.360×10^5	90.08	0.3587	1.0433	0.9982	43.28	0.3039	0.0148	1.1586	0.4201
02	0.5948		8.760×10^5	90.58	0.4917	1.0734	0.9969	43.78	0.2715	0.0148	1.2045	0.4070
03	0.7047		1.050×10^5	90.34	0.5799	1.1037	0.9950	43.54	0.2638	0.0177	1.2275	0.4062
12	0.8046		1.107×10^6	90.85	0.5968	1.1344	0.9425	44.05	0.2529	0.1656	1.1240	0.4818
13	0.7267		1.013×10^6	90.43	0.5858	1.1194	0.9938	43.63	0.2836	0.0210	1.2170	0.4217
14	0.7393		1.084×10^6	90.40	0.5923	1.1419	0.9399	43.60	0.2792	0.1190	1.1407	0.4722
15	0.7478		1.032×10^6	90.32	0.6026	1.1236	0.9909	43.52	0.2751	0.0292	1.2200	0.4207
16	0.7714		1.064×10^6	90.07	0.6103	1.1326	0.9826	43.27	0.2750	0.0535	1.2046	0.4325
20	0.7529		1.022×10^6	89.56	0.5628	1.1613	0.9887	42.76	0.3535	0.0360	1.1638	0.4726
		5° Positive Incidence										
21	0.7180	41.8	1.010×10^6	90.50	0.5821	1.1145	0.9945	43.70	0.2795	0.0189	1.2195	0.4180
		5° Negative Incidence										
30	0.4277	51.8°	6.529×10^5	90.89	0.3662	1.0313	0.9977	39.06	0.2333	0.0197	1.1182	0.3608
31	0.5987		9.008×10^5	90.98	0.5088	1.0633	0.9958	39.18	0.2349	0.0137	1.1390	0.3637
32	0.6957		1.003×10^6	91.21	0.5821	1.0903	0.9926	39.41	0.2366	0.0267	1.1452	0.3746
33	0.7545		1.068×10^6	90.66	0.6036	1.1055	0.9695	38.86	0.2301	0.0969	1.1044	0.4045
34	0.7266		1.034×10^6	91.11	0.6045	1.0959	0.9872	39.31	0.2249	0.0433	1.1427	0.3778
		10° Negative Incidence										
35	0.3574	57.9°	5.196×10^5	90.43	0.3122	1.0192	0.9983	33.43	0.2085	0.0196	1.0585	0.3168
36	0.5921		9.310×10^5	90.55	0.5137	1.0531	0.9946	33.55	0.1983	0.0255	1.0806	0.3187
37	0.7012		9.877×10^5	89.28	0.5520	1.0699	0.9766	32.28	0.1798	0.0836	1.0629	0.3315
38	0.6566		9.340×10^5	90.04	0.5682	1.0651	0.9925	33.04	0.1937	0.0297	1.0878	0.3167
40	0.6855		9.653×10^5	89.84	0.5855	1.0678	0.9852	32.84	0.1848	0.0550	1.0783	0.3232

NAVAIR SUPERCRITICAL CASCADE DATA SUMMARY

Test Point	M_1	β_1	R_E	β_2	M_2	Static Pressure Ratio P_2/P_1	Total Pressure Ratio P_{T_2}/P_{T_1}	Flow Turning $\Delta\beta$	$C_p = \frac{P_2 - P_1}{P_{T_1} - P_1}$	$\omega = \frac{P_{T_1} - P_{T_2}}{P_{T_1} - P_1}$	AVDR A_1/A_2	D_F
		3° Positive Incidence										
40	0.3957	43.8	5.875×10^5	89.09	0.3118	1.0387	0.9974	45.09	0.3394	0.0249	1.1714	0.4547
41	0.5992		8.784×10^5	89.64	0.4727	1.0884	0.9951	45.64	0.3219	0.0228	1.2204	0.4509
42	0.7046		1.016×10^6	89.87	0.5574	1.1198	0.9929	45.87	0.3051	0.0253	1.2535	0.4463
43	0.7522		1.078×10^6	89.70	0.5830	1.1385	0.9847	45.70	0.3011	0.0488	1.2441	0.4590
44	0.7937		1.140×10^6	89.80	0.5638	1.1555	0.9464	45.80	0.3021	0.1576	1.1484	0.5200
		3° Negative Incidence										
45	0.4420	49.8°	6.600×10^5	90.23	0.3695	1.0377	0.9972	40.23	0.2627	0.0223	1.1262	0.3852
46	0.6082		8.960×10^5	90.13	0.5097	1.0709	0.9959	40.13	0.2496	0.0186	1.1592	0.3790
47	0.7013		9.930×10^5	90.20	0.5861	1.0930	0.9932	40.20	0.2393	0.0244	1.1763	0.3787
48	0.7506		1.030×10^6	90.09	0.6249	1.1015	0.9868	40.09	0.2245	0.0422	1.1794	0.3790
49	0.8083		1.050×10^6	91.13	0.6374	1.0836	0.9319	41.13	0.1669	0.1950	1.0967	0.4241
		5° Positive Incidence										
56	0.4075	42°	6.320×10^5	89.73	0.3221	1.0399	0.9966	47.73	0.3293	0.0310	1.2210	0.4135
59	0.6003		9.200×10^5	90.15	0.4650	1.0920	0.9927	48.15	0.3337	0.0337	1.2473	0.4754
60	0.7055		1.064×10^6	90.26	0.5395	1.1303	0.9884	48.26	0.3307	0.0409	1.2673	0.4818
61	0.7453		8.850×10^5	90.36	0.5453	1.1438	0.9683	43.36	0.3225	0.1027	1.2212	0.5124
62	0.7538		8.970×10^5	90.60	0.5389	1.1464	0.9584	48.60	0.3200	0.1325	1.1939	0.5293
		Design Incidence										
72	0.7354	47.0	8.710×10^5	90.84	0.5604	1.1500	0.9936	43.84	0.3469	0.0213	1.1734	0.4645

LIST OF SYMBOLS, ABBREVIATIONS, AND SUBSCRIPTS

Symbols and Abbreviations

A	stream tube area
a	sound speed
AVDR	axial velocity density ratio = stream tube inlet area/exit area, A1/A2
b_x	airfoil axial chord
C	airfoil chord
Cp	static pressure rise coefficient $(P_{S2}-P_{S1})/(P_{T1}-P_1)$
D_F	diffusion factor $= (1 - W_2/W_1) + \tau/C \left[\frac{W_1 \cos \beta_1 - W_2 \cos \beta_2}{2 W_1} \right]$
M	Mach number = W/a
P	static pressure
P_T	total pressure
Re	Reynolds number based on inlet velocity and chord = WC/ν
U, V	velocity components along x, y
W	velocity
x, y	rectangular coordinates in axial and tangential directions
ω	loss coefficient = $(P_{T2}-P_{T1})/(P_{T1}-P_1)$
αs	surface chord angle
β	air angle measured from tangential
$\Delta \beta$	flow turning, $\beta_2-\beta_1$
τ	cascade gap
ν	kinematic viscosity

LIST OF SYMBOLS, ABBREVIATIONS, AND SUBSCRIPTS (Cont.'d)

Subscripts

1	cascade upstream inlet plane
2	cascade downstream exit plane
x	axial direction, engine axis
y	tangential direction

DISTRIBUTION LIST

No. of Copies	To
5	Department of the Navy, Naval Air Systems Command, Attn: AIR 310, Washington, D.C. 20361
14	Department of the Navy, Naval Air Systems Command, Attn: AIR 954, Washington, D.C. 20361
2	Office of Naval Research, Code 473, Attn: Mr. Patton 800 North Quincy Street, Arlington, VA 22217
1	Commander, Naval Air Systems Command Washington, D.C. 20361. Attn: AIR-330
1	Commander, Naval Air Systems Command Washington, D.C. 20361, Attn: AIR 330B
1	Commander, Naval Air Systems Command Washington, D.C. 20361, Attn: AIR-330C
1	Commander, Naval Air Systems Command Washington, D.C. 20361, Attn: AIR-03PA1
1	Commander, Naval Air Systems Command Washington, D.C. 20361, Attn: AIR-03PA3
1	Commander, Naval Air Systems Command Washington, D.C. 20361, Attn: AIR-530
1	Commander, Naval Air Systems Command Washington, D.C. 20361, Attn: AIR-5360
1	Commander, Naval Air Systems Command Washington, D.C. 20361, Attn: AIR-5361
1	Commanding Officer, Naval Air Propulsion Test Center Trenton, New Jersey 16828
1	Commanding Officer, Naval Air Development Center Warminster, PA 19112, Attn: AVTD
1	Melvin J. Hartman, Chief, Compressor Design Section NASA Lewis Research Center Cleveland, Ohio 44135
Remaining Copies	Prof. M. F. Platzer, Chairman Department of Aeronautics Naval Post Graduate School Monterry, CA 93940